

Optická emisní spektroskopie atomů

Diagnostické metody 1

Zdeněk Navrátil

Ústav fyziky a technologií plazmatu
Přírodovědecká fakulta Masarykovy univerzity, Brno

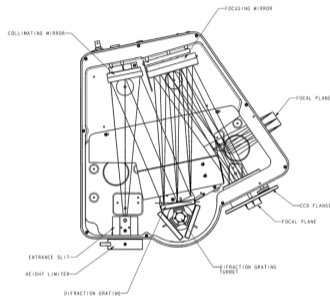
Outline

- 1 OES
- 2 CR modelling

Instrumentation

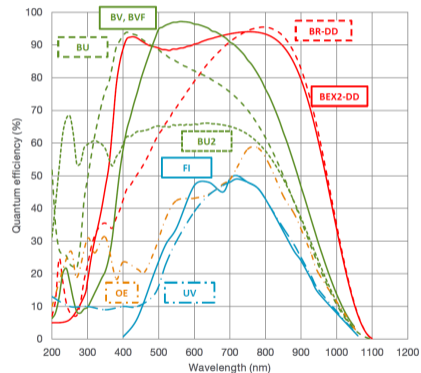
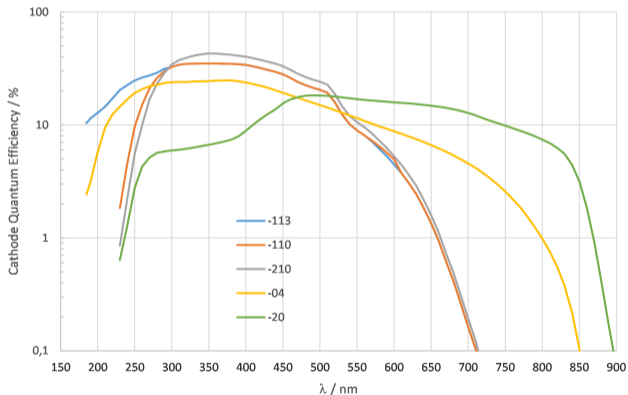
- typically grating spectrometer of Czerny-Turner mounting equipped with CCD/ICCD detector
- typical spectral range 190 – 1100 nm
- sensitivity of detectors (silicon CCD, photocathode of PMT), grating efficiency
- resolution: number of illuminated grating grooves, slit width, pixel size

$$R = \lambda / \Delta\lambda = mN$$



Sensitivities

PMC-150: Cathode Quantum Efficiency



- grating efficacy, fibre efficacy, windows

Technique overview – how we measure

- collecting the light emitted by plasma (optical emission spectroscopy, OES):
 - non-intrusive
 - sensing the light at the plasma boundary
 - optical probes
- sending the light through the plasma (optical absorption spectroscopy):
 - based on Lambert-Beer law
 - can disturb the plasma, two ports
 - white light, hollow cathode lamps, lasers
- collecting the light emitted and reabsorbed by the plasma (self-absorption methods of OES)

Technique overview – how we measure

- collecting the light emitted by plasma (optical emission spectroscopy, OES):
 - non-intrusive
 - sensing the light at the plasma boundary → self-absorption can play a role
 - optical probes
- sending the light through the plasma (optical absorption spectroscopy):
 - based on Lambert-Beer law
 - can disturb the plasma, two ports
 - white light, hollow cathode lamps, lasers
- collecting the light emitted and reabsorbed by the plasma (self-absorption methods of OES)

Technique overview – what we look at

- line positions = wavelengths: electric, magnetic fields, atom velocities (Stark, Zeeman, Doppler effect)
- lineshapes and linewidths: electron density, gas pressure, density, temperatures (Stark, van der Waals, resonance, Doppler line broadening)
- line intensities: . . . all

Technique overview – what we look at

- line positions = wavelengths: electric, magnetic fields, atom velocities (Stark, Zeeman, Doppler effect)
- lineshapes and linewidths: electron density, gas pressure, density, temperatures (Stark, van der Waals, resonance, Doppler line broadening)
- line intensities: . . . all
 - relative – instrument spectral sensitivity is taken into account, no absolute intensity calibration is performed
output: relative populations of excited states, excitation temperatures etc.
 - absolute – access to absolute densities of excited states, electron density etc.

Absolute intensity measurement

- radiant flux/zářivý tok – energy emitted/incident on surface per unit time

$$\Phi = \frac{d\mathcal{E}}{dt}, \quad \text{W} \quad (1)$$

- irradiance – flux density (per unit surface)

$$I = \frac{d\Phi}{dS} = \frac{d^2\mathcal{E}}{dt dS}, \quad \text{W m}^{-2} \quad (2)$$

- specified during calibration of calibrated light sources (spectral irradiance)
- optical fibre is not a detector of irradiance (acceptance angle)
- radiometric irradiance probes, cosine correction diffusers, integrating spheres, ...



Absolute intensity measurement 2

- radiance (zář) – radiant flux per unit perpendicular surface and unit solid angle

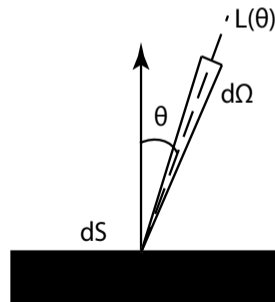
$$L = \frac{d^2\Phi}{dS \cos \theta d\Omega} = \frac{d^3\mathcal{E}}{dt dS \cos \theta d\Omega}, \quad \text{W m}^{-2} \text{sr}^{-1} \quad (3)$$

- radiance \times irradiance

$$I = \int_{\Omega} L(\theta) \cos \theta d\Omega \quad (4)$$

For constant L (Lambert) radiators $I = \pi L$.

- for description of radiating solid surfaces



Absolute intensity measurement 3

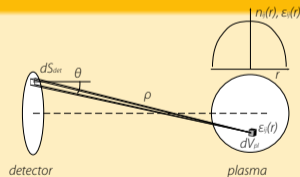
- emission coefficient – radiant power emitted by unit volume into unit solid angle

$$j = \frac{d^3 \mathcal{E}}{dt dV d\Omega} \quad (5)$$

- all quantities have their spectral densities, e.g. $j(\lambda)$

emission coefficient of transition

$$j_{ij} = \frac{1}{4\pi} n_i A_{ij} h\nu_{ij}$$



$$I_{ij} = \frac{1}{S_{det}} \int_{V_{pl}} \int_{S_{det}} \frac{j_{ij}(r)}{\rho^2} \text{Acc}(\theta) dV_{pl} dS_{det}$$

irradiation of detector for optical thin plasma condition

Electron temperature from Boltzmann plot?

- density of atoms in excited state

$$n_i = n \frac{g_i}{Q} e^{-\frac{\mathcal{E}_i}{k_b T_e}} \quad (6)$$

2 g_i – statistical weight, \mathcal{E}_i – excitation energy, n – atom density, Q – state sum, T_e excitation ($\stackrel{?}{=}$ electron) temperature

- spectral line intensity

$$I \propto n_i A_{ij} \frac{hc}{\lambda} \quad (7)$$

$$I = C \cdot \frac{g_i A_{ij}}{\lambda} e^{-\frac{\mathcal{E}_i}{k_b T_e}} \quad (8)$$

- Boltzmann plot

$$\ln \frac{I\lambda}{g_i A_{ij}} = -\frac{1}{k_b T_e} \mathcal{E}_i + \ln k_1, \quad (9)$$

Possibility of electron temperature measurement

excited level balance

- local thermodynamic equilibrium (LTE) plasma
 - LTE condition

$$n_e \gg 1.6 \cdot 10^{12} \sqrt{T_e} (\Delta E)^3 \quad (\text{cm}^{-3})$$

- electron temperature from Boltzmann plot
- non-LTE plasma
 - corona equilibrium, excitation saturation phase, ...
 - low electron density plasma
 - use of Boltzmann-plot leads to erroneous electron temperature
 - CR modelling

non-Maxwellian EDF

- inelastic collisions, beam electrons, non-local EDF

Collisional-radiative modelling

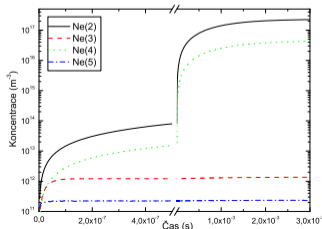
coupled DE for densities of excited states

$$\frac{\partial n_i}{\partial t} + \nabla(n_i \vec{v}) = \left(\frac{\partial n_i}{\partial t} \right)_{c,r} \quad (10)$$

population and depopulation processes are very fast:

$$\frac{\partial n_i}{\partial t} = \left(\frac{\partial n_i}{\partial t} \right)_{c,r} = 0 \quad (11)$$

not valid for ground-state atoms, ions, metastables, high pressure



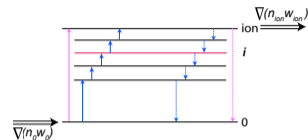
Level balance

$$\frac{\partial n_0}{\partial t} + \nabla(n_0 \vec{v}_0) = -S_{cr} n_e n_0 + \alpha_{cr} n_e n_{ion}$$

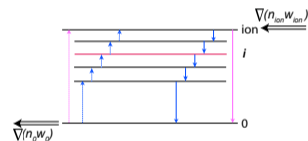
$$\frac{\partial n_{ion}}{\partial t} + \nabla(n_{ion} \vec{v}_{ion}) = +S_{cr} n_e n_0 - \alpha_{cr} n_e n_{ion}$$

classification of models (plasma state)

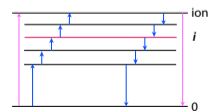
- ionizing plasma $S_{cr} n_e n_0 - \alpha_{cr} n_e n_{ion} > 0$
 - plasma conducting current, ionizing waves
- recombining plasma $S_{cr} n_e n_0 - \alpha_{cr} n_e n_{ion} < 0$
 - afterglows, outer regions of flames
- equilibrium plasma $S_{cr} n_e n_0 - \alpha_{cr} n_e n_{ion} = 0$
(ionization-recombination equilibrium)



ionizing plasma



recombining plasma

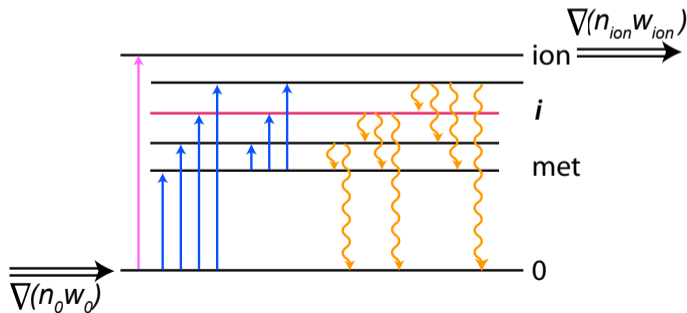


equilibrium plasma

Excitation phases: corona phase

population by electron impact excitation, radiative deexcitation

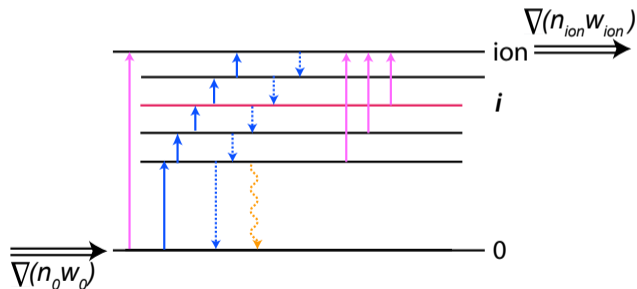
$$k_{0i}^{\text{el}} n_e n_0 + k_{mi}^{\text{el}} n_e n_m (+ \sum_{j>i} \Lambda_{ji} A_{ji} n_j) = \sum_{j<i} \Lambda_{ij} A_{ij} n_i$$



Excitation phases: excitation saturation phase

population and depopulation by electron impact

$$\sum_{j \neq i} k_{ji}^{\text{el}} n_e n_j + (\alpha_i n_e n_{\text{ion}}) = \sum_{j \neq i} k_{ij}^{\text{el}} n_e n_i + S_i n_e n_i$$

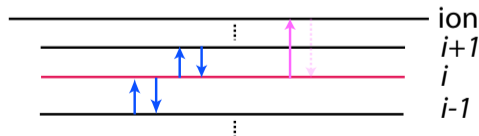


- saturation of the excited state densities with increased n_e
- no Saha equilibrium, $S_i n_i \gg \alpha_i n_{\text{ion}}$

Excitation phases: excitation saturation phase 2

- stepwise excitation \rightarrow ladder-like excitation flow
- coefficients of upward processes are larger (closer upper levels, higher statistical weights of upper levels)

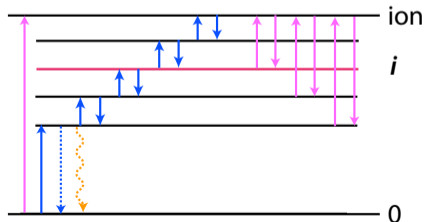
$$k_{i-1,j}n_e n_{i-1} - k_{i,j-1}n_e n_i = k_{i,j+1}n_e n_i - k_{i+1,j}n_e n_{i+1} + S_j n_e n_i$$



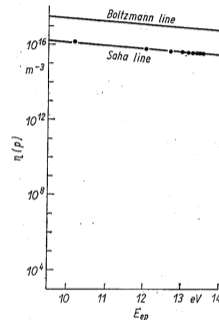
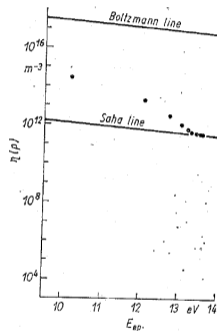
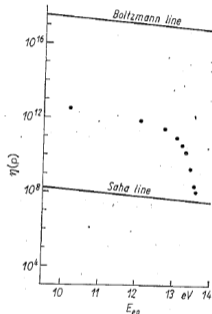
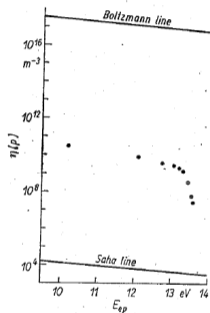
Excitation phases: partial local thermodynamic equilibrium

- 2 equilibria: excited state \times ion state, neighbouring excited states
- ionization \sim recombination \gg excitation flow

$$k_{i-1,i}n_e n_{i-1} - k_{i,i-1}n_e n_i = k_{i,i+1}n_e n_i - k_{i+1,i}n_e n_{i+1} - S_i n_e n_i + \alpha_i n_e n_{\text{ion}}$$



Role of dominant electron collisions



Boltzmann

Saha

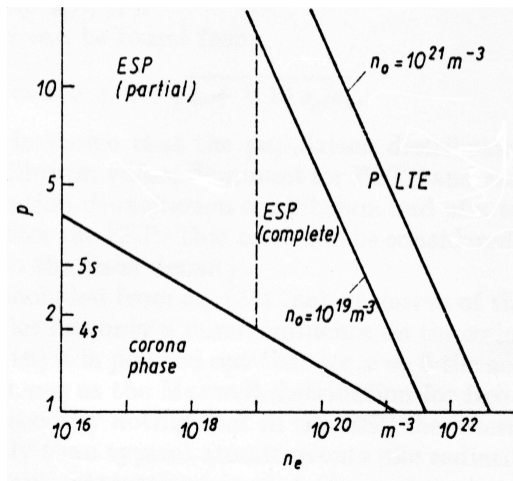
deviation from B & S

$$n_i^B = n_0 g_i / g_0 e^{-E_i / kT_e}$$

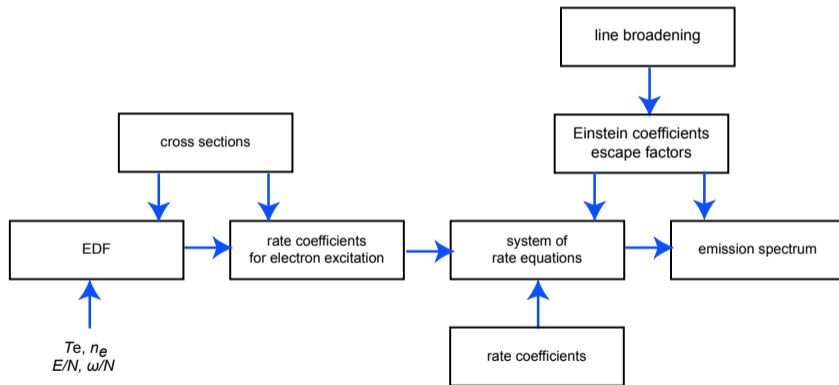
$$n_i^S = n_e n_{\text{ion}} \frac{g_i}{g_e g_{\text{ion}}} (h^2 / 2\pi m_e kT_e)^{3/2} e^{E_{\text{ion},i} / kT_e}$$

$$n_i = r_i^0 n_i^S + r_i^1 n_i^B$$

Excitation phases



Collisional-radiative model



Electron distribution function

- Maxwellian EDF
- solution of Boltzmann kinetic equation
- normalization of the EDF

$$\int_0^{\infty} f(\varepsilon) \varepsilon^{1/2} d\varepsilon = 1 \quad (12)$$

- mean electron energy

$$\langle \varepsilon \rangle = \int_0^{\infty} f(\varepsilon) \varepsilon^{3/2} d\varepsilon, \quad (13)$$

- rate coefficients k , k_{inv} of electron collision with cross section σ and of inverse process

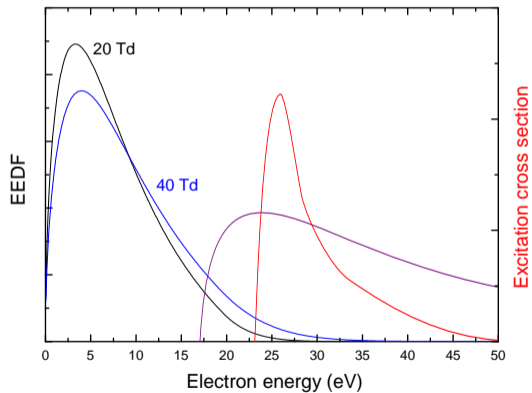
$$k = \sqrt{\frac{2e}{m_e}} \int_0^{\infty} \sigma(\varepsilon) f_0(\varepsilon) \varepsilon d\varepsilon$$

$$k_{\text{inv}} = \sqrt{\frac{2e}{m_e} \frac{g_j}{g_i}} \int_{\varepsilon_{ij}}^{\infty} \sigma(\varepsilon) f_0(\varepsilon - \varepsilon_{ij}) \varepsilon d\varepsilon$$

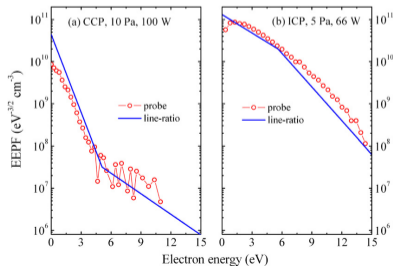
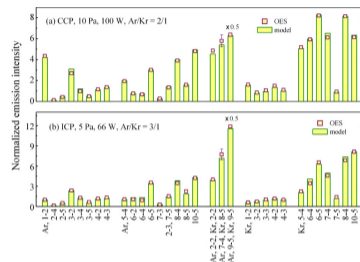
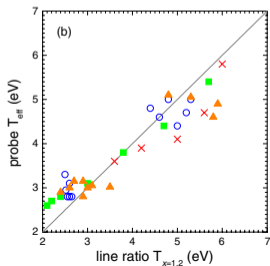
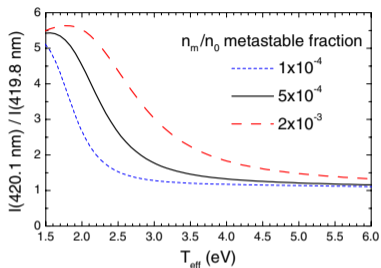
Approaches of OES data processing

- line ratio methods
 - selection of convenient line pair (sensitivity, model simplicity, ease of measurement)
 - no control of model validity
- „many line fitting“ methods

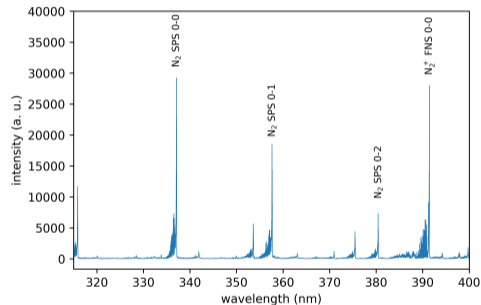
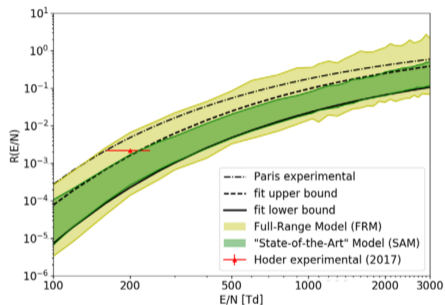
Line ratio method – ideal case



Electron temperature and EDF measurement by OES+CR



Electric field measurement in air



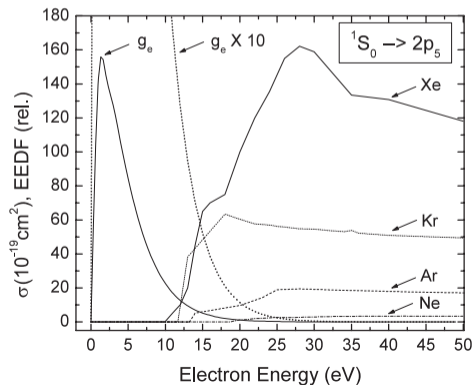
$$R(E/N) = \frac{FNS(0,0)}{SPS(0,0)}$$

Kozlov and Wagner 2001 *J. Phys. D: Appl. Phys.* **34** 3164

Bilek et al 2018 *Plasma Sources Sci. Technol.* **27** 085012

TRG spectroscopy

- based on admixing of a small amount of rare gas into plasma
- mapping EDF at specific electron energies
- low pressure, what is small amount?



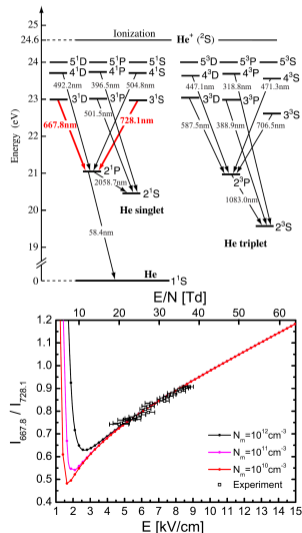
Helium line ratio method

- ratio of helium singlet lines $R = I_{667}/I_{728}$
 He I 667.8 nm ($2^1P - 3^1D$)
 He I 728.1 nm ($2^1P - 3^1S$)
- ✓ high spectral resolution is not required
- ✓ sensitive to fields of several kV/cm
- ✓ verified at atmospheric pressure
- ✗ dependence on the gas purity
- ✗ dependence on metastable density at low field

$$E(R) = 2.224 - 20.18R + 45.07R^2 - 19.98R^3 + 3.369R^4$$

$[E] = \text{kV/cm}$, for 3–40 kV/cm, $T = 310 \text{ K}$

Ivković et al 2014 *J. Phys. D: Appl. Phys.* 47 055204



Diffuse coplanar barrier discharge in rare gases

Neon



diffuse,
high gas purity

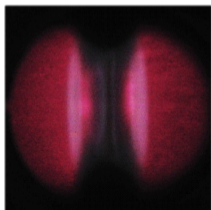


filamentary,
low gas purity

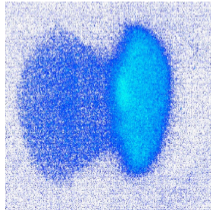
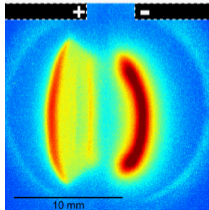


low gas purity,
higher voltage

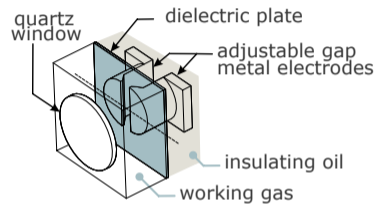
Helium



50 ms

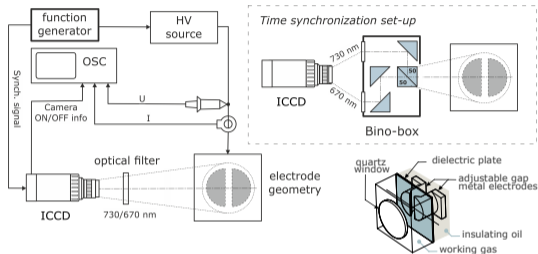
1 μ s

100 ns, 10 k



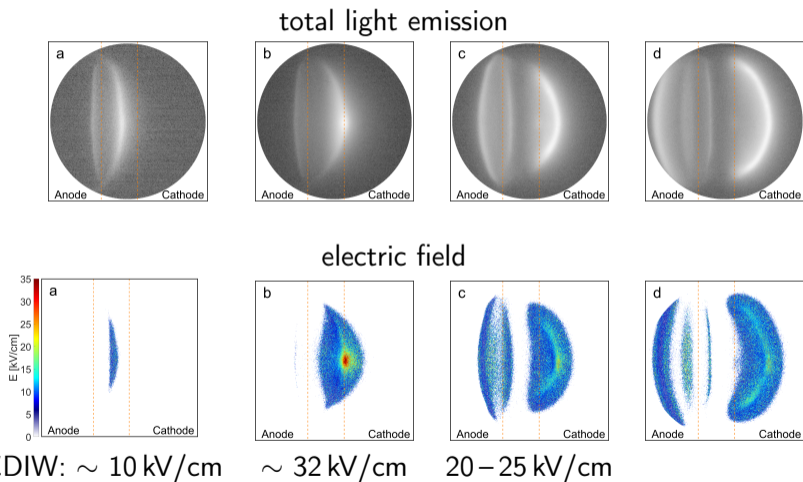
run: I.mp4

Experimental setup



- coplanar DBD, brass electrodes covered with 96% Al_2O_3 (0.63 mm thick),
- parallel gap footprint, electrode distance 4.75 mm,
- helium 5.0 at atmospheric pressure, gas flow 550 sccm
- AC sine-wave high voltage of 1.6 kVmax, 10.3 kHz
- ICCD camera Princeton Instruments PI-MAX3 (time window 50 ns)
- bandpass filters Thorlabs FL670-10 and FL730-10 (670, 730 nm, FWHM 10 nm)

2D resolved electric field development



2D resolved simultaneous line ratio measurement

